1446, 1411, 1082, 996 cm^{-1}; ^{1}H NMR (in $CDCl_3$) δ 0.79–1.00 (m, 15 H, EtSi), 3.55 (s, 3 H, MeO), 4.42 (quint, 1 H, HSi, J = 3.3 Hz), 5.81 (dd, 1 H, vinylic proton, J_{trans} = 20.1, J_{gem} = 3.9 Hz), 6.14 (dd, 1 H, vinylic proton, J_{cis} = 15.2, J_{gem} = 3.9 Hz), 6.45 (dd, 1 H, vinylic proton, J_{trans} = 20.1, J_{cis} = 15.2 Hz), 7.31–7.67 (m, 4 H, ring protons); ^{13}C NMR (in $CDCl_3$) δ 4.37, 6.34, 6.87, 8.36 (EtSi), 50.8 (MeO), 128.2, 128.4, 135.1, 135.6, 142.3, 142.8 (ring carbons), 134.7 (CH_2=CH), 135.3 (CH=CH_2); ^{29}Si NMR (in $CDCl_3$) δ −7.48, −2.55. Anal. Calcd for $C_{15}H_{26}OSi_2$: C, 64.68; H, 9.40. Found: C, 64.68; H, 9.39.

Photolysis of 1 in the Presence of Benzaldehyde. A mixture of 0.3456 g (1.39 mmol) of 1, 0.7498 g (7.07 mmol) of benzaldehyde, and 0.1186 g (0.645 mmol) of tridecane in 20 mL of hexane was photolyzed for 2 h. The mixture was analyzed by GLC as being compound 11 (27% yield), along with 60% starting compound 1. Compound 11 was isolated by preparative GLC: ^{1}H NMR (in $CDCl_3$) δ 0.36–1.09 (m, 20 H, EtSi), 5.18 (s, 1 H, HC), 7.30–7.55 (m, 9 H, phenyl and phenylene ring protons).[8] Other spectral data obtained from 11 were identical with those of the authentic sample.[1]

Photolysis of 1 in the Absence of a Trapping Agent with a High-Pressure Mercury Lamp Bearing a Pyrex Filter. A mixture of 0.5253 g (2.12 mmol) of 1 and 0.1169 g (0.635 mmol) of tridecane in 60 mL of hexane was photolyzed with a high-pressure mercury lamp bearing a Pyrex filter for 3 h. GLC analysis of the mixture showed that 100% of starting compound 1 was recovered unchanged.

Photolysis of 1 in the Presence of *tert*-Butyl Alcohol with a High-Pressure Mercury Lamp Bearing a Pyrex Filter. A mixture of 0.6064 g (2.45 mmol) of 1, 0.4985 g (6.74 mmol) of *tert*-butyl alcohol, and 0.1145 g (0.622 mmol) of tridecane in 60 mL of hexane was photolyzed with a high-pressure mercury lamp bearing a Pyrex filter for 3 h. GLC analysis of the mixture showed that 100% 1 was recovered unchanged.

Photolysis of 1 in the Presence of Acetophenone with a High-Pressure Mercury Lamp Bearing a Pyrex Filter. A mixture of 0.6249 g (2.52 mmol) of 1, 1.1800 g (9.83 mmol) of acetophenone, and 0.1189 g (0.646 mmol) of tridecane in 60 mL of hexane was photolyzed for 1 h. The mixture was analyzed by GLC as being 8 (79% yield), in addition to 19% starting compound 1. Compound 8 was isolated by preparative GLC: MS *m/e* 368 (M^{+}); IR ν 1598, 1491, 1459, 1414, 1378, 1367, 1236, 1120 cm^{-1}; ^{1}H NMR (in $CDCl_3$) δ 0.19–1.15 (m, 20 H, EtSi), 1.72 (s, 3 H, Me), 7.13–7.58 (m, 9 H, ring protons); ^{13}C NMR (in $CDCl_3$) δ 1.71, 3.85, 7.08, 7.12, 7.21, 7.78, 8.07, 8.65 (EtSi), 27.8 (Me), 72.5 (CO), 124.3, 125.1, 127.9, 128.2, 128.3, 132.9, 134.7, 141.4, 143.9, 148.2 (ring carbons); ^{29}Si NMR (in $CDCl_3$) δ −6.50, 2.48. Anal. Calcd for $C_{22}H_{32}OSi_2$: C, 71.68; H, 8.75. Found: C, 71.65; H, 8.75.

Photolysis of 1 in the Presence of Benzaldehyde with a High-Pressure Mercury Lamp Bearing a Pyrex Filter. A mixture of 0.5371 g (2.17 mmol) of 1, 1.6769 g (15.8 mmol) of benzaldehyde, and 0.1786 g (0.971 mmol) of tridecane as an internal standard in 60 mL of hexane was photolyzed for 45 min. GLC analysis of the mixture showed the presence of 11 in 67% yield, along with 23% starting compound 1. Compound 11 was isolated by preparative GLC. All spectral data obtained from 11 were identical with those of the authentic sample.

Acknowledgment. This research was supported in part by a Grant-in-Aid for Scientific Research on Priority Area of Organic Unusual Valency, No. 3233105, from the Ministry of Education, Science and Culture. We thank Shin-Etsu Chemical Co. Ltd., Nitto Electric Industrial Co. Ltd., Dow Corning Japan Ltd., and Toshiba Silicone Co. Ltd. for financial support.

Registry No. 1, 135888-05-0; 2, 141586-14-3; 3a, 135888-09-4; 3b, 141586-15-4; 6, 141586-16-5; 7, 141586-17-6; 8, 141586-18-7; 9, 135888-14-1; 10, 141586-19-8; 11, 135888-13-0; AcPh, 98-86-2.

OM910807N

---

[8] We reported the chemical shift of EtSi protons for 11 as 0.98–1.09 ppm, but this is incorrect. The correct chemical shift should be 0.36–1.09 ppm as reported here.

Synthesis, Characterization, and Properties of 16-Electron Cp*M(NO)(aryl)$_2$ (M = Mo, W) Complexes[1]

Neil H. Dryden, Peter Legzdins,* Steven J. Rettig, and John E. Veltheer

Department of Chemistry, The University of British Columbia, Vancouver, British Columbia, Canada V6T 1Z1

Received January 30, 1992

Treatment of Cp*M(NO)Cl_2 (Cp* = η^5-C_5Me_5; M = Mo, W) in THF at low temperatures with equimolar amounts of diarylmagnesium reagents, (aryl)$_2$Mg·*x*(dioxane), affords the diaryl complexes Cp*M(NO)(aryl)$_2$ (aryl = Ph, *o*-tolyl, or *p*-tolyl), which are isolable in moderate yields and have been fully characterized by conventional spectroscopic methods. In addition, single-crystal X-ray crystallographic analyses have been performed on both *o*-tolyl complexes. Crystal data for Cp*Mo(NO)(*o*-tolyl)$_2$ (3): a = 11.570 (2) Å, b = 10.128 (3) Å, c = 18.439 (4) Å, β = 92.50 (2)°, Z = 4, space group $P2_1/a$ (No. 14), R_F = 0.030, R_{wF} = 0.033 for 3387 reflections with $I \geq 3\sigma(I)$. Crystal data for Cp*W(NO)(*o*-tolyl)$_2$ (6): a = 11.612 (3) Å, b = 10.168 (5) Å, c = 18.250 (3) Å, β = 91.87 (2)°, Z = 4, space group $P2_1/a$ (No. 14), R_F = 0.037, R_{wF} = 0.040 for 3019 reflections with $I \geq 3\sigma(I)$. Complexes 3 and 6 are isostructural and isomorphous and possess three-legged piano-stool molecular structures. Their intramolecular metrical parameters are comparable to those exhibited by the related dialkyl complex CpW(NO)(CH_2SiMe_3)$_2$, the most notable difference being the C_{aryl}–M–C_{aryl} angle in both 3 and 6, which is significantly greater than the C_{alkyl}–M–C_{alkyl} angle in the dialkyl species. The IR and electrochemical properties of the Cp*M(NO)(aryl)$_2$ complexes indicate that their metal centers are more electron deficient than those in comparable Cp′M(NO)(alkyl)$_2$ (Cp′ = Cp (η^5-C_5H_5), Cp*; M = Mo, W) complexes. This greater Lewis acidity is also manifested by the increased stability of the 1:1 adducts formed between the diaryl complexes and typical Lewis bases.

Introduction

Previous work in our laboratories resulted in the discovery of a family of 16-electron dialkyl complexes having the general formula CpW(NO)R_2 (Cp = η^5-C_5H_5; R = alkyl = CH_2SiMe_3, CH_2CMe_3, CH_2CMe_2Ph).[2] A surprising property of these formally unsaturated compounds is their thermal and oxidative stability. For example, they may be handled as solids in air for short periods of time at ambient temperatures with no deleterious effects, although

---

[1] Organometallic Nitrosyl Chemistry. 53. Part 52: Reference 28.

[2] Legzdins, P.; Rettig, S. J.; Sánchez, L.; Bursten, B. E.; Gatter, M. G. *J. Am. Chem. Soc.* 1985, *107*, 1411.

0276-7333/92/2311-2583$03.00/0

exposure to O_2 for several days at 25 °C converts them to oxo complexes.[3] The results of Fenske–Hall MO calculations on the model complexes $CpM(NO)Me_2$ (M = Mo,[2] W[4]) indicate that their LUMO's are metal-centered and are nonbonding in nature. Therefore, there is no loss of metal–ligand binding or stability in $CpM(NO)Me_2$ and related complexes despite their formal electron deficiency.

The characteristic reactivity of this family of dialkyl complexes was investigated using $CpW(NO)(CH_2SiMe_3)_2$ as a prototype.[5] The existence of the metal-centered LUMO's confers Lewis acid properties on the $Cp'M(NO)R_2$ complexes (Cp′ = Cp, Cp*(η^5-C_5Me_5)). Hence, in addition to forming isolable 1:1 adducts with Lewis bases (e.g. $PMe)_3$, they react with other small molecules (e.g. CNR′, NO, O_2, etc.) in a manner which reflects initial adduct formation followed by subsequent intramolecular transformations involving the alkyl ligands.[5] In general, the molybdenum complexes are more reactive than are their tungsten congeners.

Logically, we wished to extend this family of alkyl nitrosyl compounds to encompass related aryl complexes. It was our expectation that the characteristic chemistry exhibited by these new $Cp'M(NO)(aryl)_2$ species would be dependent on the nature of the aryl group. Such behavior has been documented in the related family of complexes $Cp^*Ru(NO)R_2$, for which Bergman and co-workers have established differences in the comparative reactivity of the alkyl- versus aryl-substituted complexes,[6,7] e.g.

$$Cp^*Ru(NO)Me_2 + 2PMe_3 \xrightarrow{\Delta} Cp^*Ru(CN)(PMe_3)_2 + H_2O + CH_4 \quad (1)$$

$$Cp^*Ru(NO)Ph_2 + 2PMe_3 \xrightarrow{\Delta} Cp^*Ru(NO)(PMe_3)_2 + Ph\text{–}Ph \quad (2)$$

Furthermore, it was probable that the metal centers in the $Cp'M(NO)(aryl)_2$ complexes would be less sterically hindered than in their dialkyl analogues, thereby enhancing the reactivity of the diaryl complexes toward larger Lewis base substrates.

Originally, the dialkyl nitrosyl complexes were prepared by the sequential treatment of $CpW(NO)I_2$ with RMgCl in Et_2O at room temperature followed by hydrolysis of the intermediate isonitrosyl adducts as summarized in eqs 3 and 4.[5,8] Very early on we discovered that the synthetic

$$2CpW(NO)I_2 + 4RMgCl \rightarrow [Cp'W(NO)R_2]_2{\cdot}MgICl + 3MgICl \quad (3)$$

$$[Cp'W(NO)R_2]_2{\cdot}MgICl + H_2O\ (\text{excess}) \rightarrow 2Cp'W(NO)R_2 + \text{insoluble Mg salts} \quad (4)$$

methodology employed to prepare the dialkyl complexes (eqs 3 and 4) cannot be used to synthesize the analogous diaryl complexes because water in the second step is simply disastrous. Indeed, all $Cp'M(NO)(aryl)_2$ complexes synthesized in our laboratories to date react instantaneously with H_2O at ambient temperatures.[9,10] Furthermore, the choices of solvent, reaction temperature, and dihalo starting material for the alkyl complexes were inappropriate for the synthesis of diaryl complexes.

Given that the previous synthetic methodology could not be extended to include the diaryl complexes, we therefore had good reason to develop a new set of experimental conditions and reagents to synthesize these compounds. In this paper we describe the preparation and isolation of six new $Cp^*M(NO)(aryl)_2$ (M = Mo, W; aryl = phenyl, *p*-tolyl, *o*-tolyl) complexes which have been fully characterized by conventional spectroscopic methods. In addition, the solid-state molecular structures of both $Cp^*M(NO)(o\text{-tolyl})_2$ compounds have been established by single-crystal X-ray crystallography.

Experimental Section

All reactions and subsequent manipulations involving organometallic reagents were performed under anhydrous conditions under an atmosphere of prepurified argon. Conventional drybox and vacuum line Schlenk techniques[11,12] were utilized throughout. The organometallic reagents $Cp^*M(NO)Cl_2$ (M = Mo, W) were prepared by established procedures.[13] $Cp^*Mo(NO)Cl_2$ was recrystallized by Soxhlet extraction with CH_2Cl_2, and $Cp^*W(NO)Cl_2$ was stored at −30 °C and used within 1 month of preparation. The various aryl halide reagents (i.e. chlorobenzene, *p*-chlorotoluene, and *o*-chlorotoluene) were purified by distillation from P_2O_5 under reduced pressure.[14] PhMgCl, (*p*-tolyl)MgCl, and (*o*-tolyl)MgCl (1.0 M in THF) were purchased from Aldrich Chemical Co. and were used as received. Activated magnesium powder was obtained from Baker Scientific. Solvents were freshly distilled from appropriate drying agents under a dinitrogen atmosphere and were either purged for 10 min with argon prior to use or were directly vacuum-transferred from the appropriate drying agent. Dioxane, tetrahydrofuran, and diethyl ether were distilled from sodium/benzophenone; hexanes and pentane were distilled from sodium/benzophenone/tetraglyme; dichloromethane was doubly distilled from P_2O_5; toluene was distilled from sodium.[14]

All IR samples were either as THF solutions in NaCl cells or as Nujol mulls sandwiched between NaCl plates. IR spectra were recorded on a Nicolet 5DX FT-IR instrument, internally calibrated with a He/Ne laser. All ^1H NMR spectra were obtained on a Varian Associates XL-300 spectrometer, and the chemical shifts of the observed resonances are reported in parts per million downfield from Me_4Si referenced to the residual proton signal of C_6D_6 (δ 7.15). Mrs. M. T. Austria, Ms. L. K. Darge, and Dr. S. O. Chan assisted in obtaining the NMR data. Low-resolution mass spectra (EI, 70 eV) were recorded on a Kratos MS50 spectrometer using the direct-insertion method by Dr. G. K. Eigendorf and Mr. M. A. Lapawa. All elemental analyses were performed by Mr. P. Borda of this department.

General Preparation of $R_2Mg{\cdot}x$(Dioxane). A general procedure for the preparation of diarylmagnesium reagents is outlined below; this methodology is a modification of the published procedure for the preparation of unsolvated dialkylmagnesium complexes.[15] The method presented below was utilized to synthesize $(Ph)_2Mg{\cdot}x$(dioxane), (*p*-tolyl)$_2Mg{\cdot}x$(dioxane), and (*o*-tolyl)$_2Mg{\cdot}x$(dioxane) which were used in this work.

A 0.4 M solution of the Grignard reagent in THF was prepared (either from activated Mg powder and aryl chloride or by dilution of purchased RMgCl solution). The solution was then treated with 1,4-dioxane (2.2 equiv diluted with 2 parts THF) dropwise from an addition funnel. The resulting white slurry was stirred for 6–24 h at room temperature to obtain a thick white slurry of

---

[3] Legzdins, P.; Phillips, E. C.; Sánchez, L. *Organometallics* 1989, *8*, 940.

[4] Bursten, B. E.; Cayton, R. H. *Organometallics* 1987, *6*, 2004.

[5] Legzdins, P.; Rettig, S. J.; Sánchez, L. *Organometallics* 1988, *7*, 2394.

[6] Seidler, M. D.; Bergman, R. G. *J. Am. Chem. Soc.* 1984, *106*, 6110.

[7] Chang, J.; Bergman, R. G. *J. Am. Chem. Soc.* 1987, *109*, 4298.

[8] Hunter, A. D.; Legzdins, P.; Martin, J. T.; Sánchez, L. *Organomet. Synth.* 1986, *3*, 66.

[9] Legzdins, P.; Lundmark, P. J.; Phillips, E. C.; Rettig, S. J.; Veltheer, J. E. *Organometallics*, in press.

[10] A particularly striking example of this reactivity is provided by our recent discovery of water converting one of these diaryl nitrosyl compounds to its arylimido oxo analogue: Legzdins, P.; Rettig, S. J.; Ross, K. J.; Veltheer, J. E. *J. Am. Chem. Soc.* 1991, *113*, 4361.

[11] Shriver, D. F.; Drezdzon, M. A. *The Manipulation of Air-Sensitive Compounds*, 2nd ed.; Wiley-Interscience: New York, 1986.

[12] Wayda, A. L.; Darensbourg, M. Y. *Experimental Organometallic Chemistry: A Practicum in Synthesis and Characterization*; ACS Symposium Series 357; American Chemical Society: Washington, DC, 1987.

[13] Dryden, N. H.; Legzdins, P.; Batchelor, R. J.; Einstein, F. W. B. *Organometallics* 1991, *10*, 2077.

[14] Perrin, D. D.; Armarego, W. L. F.; Perrin, D. R. *Purification of Laboratory Chemicals*, 3rd ed.; Pergamon Press: Oxford, England, 1988.

[15] (a) Anderson, R. A.; Wilkinson, G. *J. Chem. Soc., Dalton Trans.* 1977, 809. (b) Anderson, R. A.; Wilkinson, G. *Inorg. Synth.* 1979, *19*, 262.

Table I. Numbering Scheme, Color, Yield, and Elemental Analysis Data for Complexes 1–7

complex	compd. no.	color (yield, %)	anal. found (calcd) C	H	N
Cp*Mo(NO)Ph$_2$^{a}	1	violet (42)	60.51 (63.61)	5.87 (6.07)	3.19 (3.37)
Cp*Mo(NO)(*p*-tolyl)$_2$	2	purple (65)	64.83 (65.01)	6.70 (6.59)	2.92 (3.16)
Cp*Mo(NO)(*o*-tolyl)$_2$	3	purple (32)	65.06 (65.01)	6.57 (6.59)	3.16 (3.16)
Cp*W(NO)Ph$_2$	4	blue (55)	52.30 (52.50)	5.00 (5.01)	2.66 (2.78)
Cp*W(NO)(*p*-tolyl)$_2$	5	blue (81)	53.98 (54.25)	5.52 (5.50)	2.62 (2.63)
Cp*W(NO)(*o*-tolyl)$_2$	6	violet (40)	55.15 (54.25)	5.89 (5.50)	2.59 (2.63)
Cp*W(NO)(*p*-tolyl)$_2$(PMe$_3$)	7	white (80)	53.43 (53.39)	6.22 (6.31)	2.30 (2.31)

^{a}The elemental analyses of C, H, and N are proportionally low due to a small quantity of residual MgCl$_2$, which could not be removed without decomposing the organometallic complex.

insoluble MgCl$_2$·(dioxane). The supernatant solution containing the desired R$_2$Mg·*x*(dioxane) was isolated by centrifuging portions of the slurry for 20 min at 3500 rpm and then removing the clear supernatant solutions by cannulation. The solvent was removed from the combined supernatant solutions under reduced pressure to obtain tarry residues. These residues were triturated exhaustively with hexanes, the hexanes being carefully removed after each trituration by cannulation. The remaining solid was dried in vacuo (5 × 10^{-3} Torr for 24 h at 25 °C) to obtain the organomagnesium products as dusty white pyrophoric powders. Higher purity diarylmagnesium reagents were prepared by recrystallization of these powders from THF/Et$_2$O containing a small amount of excess dioxane. The compositions of the powders or crystals with respect to their active carbanion equivalents were established by hydrolysis of weighed solid samples and titration of the resulting solutions with 0.100 N HCl using phenolphthalein as the indicator.

Preparation of Cp*M(NO)(aryl)$_2$ (M = Mo, W; aryl = Ph, *p*-tolyl, *o*-tolyl; 1–6). Since the synthetic approach to each of these six complexes is similar, their syntheses are presented in a generalized manner.

Solid Cp*M(NO)Cl$_2$ (2.00 mmol) and solid R$_2$Mg·*x*(dioxane) (1.98 mmol) were intimately mixed in a Schlenk tube contained in a glovebox. The tube was removed from the box and was attached to a vacuum line, whereupon THF (25 mL) was vacuum-transferred onto the solids at −196 °C. The reaction mixture was then warmed to −50 °C under an atmosphere of argon. After being stirred for 30 min at −50 °C, the mixture was warmed to 0 °C. The solvent was removed in vacuo *without* further warming of the reaction mixture, and the residues were washed with pentane. The dried blue to purple residues were then extracted with cold Et$_2$O (10 °C) and the extracts filtered through Celite (4 × 15 cm) at −20 °C supported on a sintered-glass frit.[16] The extracts were concentrated in vacuo until the first signs of crystallization were evident.[17] Complete crystallization occurred upon storing the concentrated extracts in a freezer overnight. Finally, the desired diaryl complex was isolated by removal of the supernatant solution by cannulation and drying of the remaining crystals in vacuo.

The tungsten complexes 4–6 are more stable than the molybdenum complexes 1–3 and can therefore be filtered through Florisil (60–100 mesh) maintained at low temperatures rather than Celite as specified above. However, transfer of the THF by syringe or the use of Grignard reagents in THF as the arylating agents reduces the isolated yields of products by 20–30%.[18] The physical properties of 1–6 are collected in Tables I–III.

Table II. Mass Spectral and Infrared Data for Complexes 1–7

compd. no.	MS, *m/z*^{a}	temp,^{b} °C	IR, cm^{-1} ν_{NO} (THF)	ν_{NO} (Nujol)
1	417 [P$^+$]	90	1615	1592
2	445 [P$^+$] 415 [P$^+$ − NO]	100	1609	1603
3	445 [P$^+$] 415 [P$^+$ − NO]	80	1601	1587
4	503 [P$^+$]	120	1588	1576
5	531 [P$^+$]	100	1582	1576
6	531 [P$^+$] 439 [P$^+$ − toluene]	80	1601	1545
7	531 [P$^+$ − PMe$_3$]^c	180	1562	1559

^{a}*m/z* values are for the highest intensity peak of the calculated isotopic cluster, i.e. ^{98}Mo and ^{184}W. ^{b}Probe temperatures. ^{c}FAB-MS (matrix 3-nitrobenzyl alcohol) revealed a parent ion of 607.

Table III. ^{1}H NMR Data for Complexes 1–7

compd. no.	^{1}H NMR (C$_6$D$_6$), δ
1	7.81 (dd, 4 H, *J* = 7.2, 1.2 Hz, ortho protons)
	7.23 (t, 4 H, *J* = 7.2 Hz, meta protons)
	7.12 (t, 2 H, *J* = 7.2 Hz, para protons)
	1.59 (s, 15 H, C$_5$(C*H*$_3$)$_5$)
2	7.77 (d, 4 H, *J* = 6.9 Hz, aryl protons)
	6.98 (d, 4 H, *J* = 6.9 Hz, aryl protons)
	2.07 (s, 6 H, 2 × Me)
	2.59 (s, 15 H, C$_5$(C*H*$_3$)$_5$)
3	7.25–6.94 (m, 8 H, aryl protons)
	2.20 (s, 6 H, 2 × Me)
	1.60 (s, 15 H, C$_5$(C*H*$_3$)$_5$)
4	7.99 (d, 4 H, *J* = 8.0 Hz, ortho protons)
	7.18 (t, 4 H, *J* = 7.4 Hz, meta protons)
	7.07 (d, 2 H, *J* = 7.2 Hz, para protons)
	1.58 (s, 15 H, C$_5$(C*H*$_3$)$_5$)
5	8.01 (d, 4 H, *J* = 6.4 Hz, ortho protons)
	6.99 (d, 4 H, *J* = 6.4 Hz, meta protons)
	2.01 (s, 6 H, 2 × Me)
	1.65 (s, 15 H, C$_5$(C*H*$_3$)$_5$)
6	7.88–7.00 (m, 8 H, aryl protons)
	2.92 (s, 6 H, 2 × Me)
	1.62 (s, 15 H, C$_5$(C*H*$_3$)$_5$)
7^b	7.86 (dm, 2 H, 2 of 4 ortho protons, transoidal to PMe$_3$)^a
	7.07 (d, 2 H, *J* = 7.1 Hz, 2 of 4 meta protons)
	6.99 (d, 2 H, *J* = 7.1 Hz, 2 of 4 ortho protons)
	6.91 (d, 2 H, *J* = 7.1 Hz, 2 of 4 meta protons)
	2.23 (s, 6 H, 2 × Me)
	1.48 (s, 15 H, C$_5$(C*H*$_3$)$_5$)
	0.59 (d, 9 H, *J* = 9.5 Hz, P(C*H*$_3$)$_3$)

^{a}J_{HP} not resolved. ^{b}^{31}P NMR (C$_6$D$_6$): δ −21.11.

Attempts to prepare the analogous CpMo(NO)(aryl)$_2$ (aryl = Ph, *o*-tolyl, *p*-tolyl) and CpW(NO)(aryl)$_2$ (aryl = Ph, *p*-tolyl) complexes via methodology similar to that outlined above have so far been unsuccessful.[19] Reaction of CpM(NO)Cl$_2$ complexes with the appropriate diarylmagnesium reagents in THF results in distinctive red-purple to blue solutions. The IR spectra of these reaction solutions show strong bands in the region anticipated for the ν_{NO} signals of these diaryl complexes: CpMo(NO)(*o*-tolyl)$_2$, 1624 cm^{-1}; CpW(NO)Ph$_2$, 1601 cm^{-1}; CpW(NO)(*p*-tolyl)$_2$, 1599 cm^{-1}. However, all attempts to isolate the these aryl complexes have resulted in a rapid color change to red-brown and loss of their distinctive IR spectral features. Unfortunately, solutions of these diaryl species cannot be treated with trapping reagents to obtain isolable products. For example, a THF solution of CpMo(NO)(*p*-tolyl)$_2$ (1 mmol generated in situ) was treated with PMe$_3$ (1 atm) at −50 °C. The deep violet color characteristic of CpMo(NO)(*p*-tolyl)$_2$ was instantly consumed, leaving an amber

---

[16] The requisite low-temperature frit for performing this operation is available from Kimble Science Products under the Kontes trademark.

[17] If brown solids appeared on the sides of the flask during the initial concentration procedure, a second low-temperature filtration was done.

[18] Commercially available aryl Grignard reagents contain residual aryl halide, as well as Wurtz coupling products, which complicate the purification and isolation of the desired organometallic products.

[19] CpW(NO)(*o*-tolyl)$_2$ has, however, been prepared in moderate yields in this manner.[10]

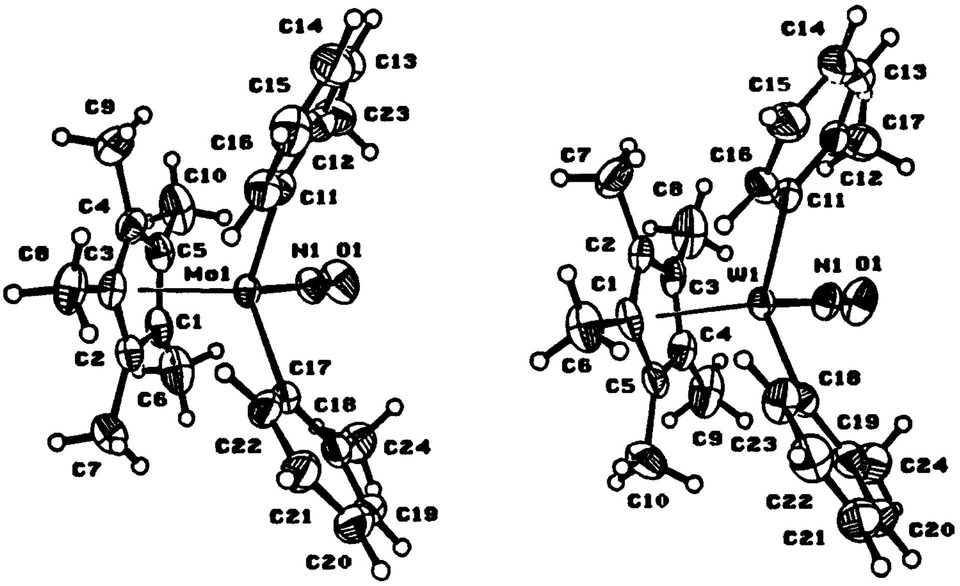

Figure 1. Views of the solid-state molecular structures of Cp*Mo(NO)(*o*-tolyl)$_2$ (**3**; left) and Cp*W(NO)(*o*-tolyl)$_2$ (**6**; right). Probability ellipsoids at the 33% level are shown for the non-hydrogen atoms.

solution which was taken to dryness in vacuo. The brown residue was suspended in Et$_2$O (100 mL) and filtered through alumina I (2 × 5 cm) supported on a sintered-glass frit. The column was washed with Et$_2$O (2 × 50 mL). The yellow filtrate was taken to dryness and dissolved in C$_6$D$_6$ to yield an amber solution. A ^{1}H NMR spectrum revealed 4,4′-dimethylbiphenyl (δ 7.45 d, 7.03 d, 2.16 s) to be the major product in the mixture. An unidentified Cp peak at δ 5.24 quickly diminished in intensity as new spectra were recorded. Within 30 min the peak at δ 5.24 was gone and the walls of the NMR tube were coated with an insoluble dark brown precipitate. The only two identifiable compounds left in solution at that time were PMe$_3$ and 4,4′-dimethylbiphenyl.

Preparation of Cp*W(NO)(*p*-tolyl)$_2$(PMe$_3$) (7). A sample of Cp*W(NO)(*p*-tolyl)$_2$ (35 mg, 0.066 mmol) was dissolved in hexanes (10 mL) at room temperature. PMe$_3$ (1 atm) was introduced into the Schlenk tube via vacuum transfer from Na/benzophenone, whereupon the deep blue solution instantly became yellow. Concentration and cooling overnight at −30 °C induced the precipitation of a white powder, which was collected and washed with cold pentane (5 mL) to obtain analytically pure Cp*W(NO)(*p*-tolyl)$_2$(PMe$_3$) (32 mg, 80%). The physical properties of this complex are also contained in Tables I–III.

Preparation and Characterization of Cp*W(NO)(CH$_2$CMe$_2$Ph)$_2$. Since the electrochemistry of this previously unreported dialkyl complex is compared to that of complex **5** later in this paper, we present its preparation and characterization here.

A solution of Cp*W(NO)Cl$_2$ (0.840 g, 2.00 mmol) in THF (40 mL) was cooled to −50 °C. A THF (20 mL) solution of (PhMe$_2$CCH$_2$)$_2$Mg·*x*(dioxane) (0.910 g, 4.00 mmol of PhMe$_2$CCH$_2^-$, prepared in a manner similar to that for (aryl)$_2$Mg·*x*(dioxane)), was then cannulated into the cooled solution of the dichloride complex, causing an immediate color change from green to red-purple. The mixture was stirred for 1 h, whereupon the solvent was removed in vacuo. Pentane (50 mL) was added to the residue. The resulting red slurry was stirred for 30 min, and the pentane was then removed in vacuo. The oily red residue was extracted with benzene (15 mL) and transferred to the top of a Florisil column (2 × 8 cm), and a single red-orange band was eluted and collected using benzene as eluant. The volume of the eluate was reduced to 5 mL, and the chromatographic procedure was repeated. The benzene solvent was then removed, and the resulting red oil was dissolved in hexanes. The volume of the solvent was reduced until the first signs of crystallization were evident, and the solution was placed in a freezer to complete the crystallization. After 1 week the mother liquor was removed from clusters of red needles of Cp*W(NO)(CH$_2$CMe$_2$Ph)$_2$ (0.50 g, 40%). Attempts to obtain further fractions of product from the mother liquor were unsuccessful. Anal. Calcd for C$_{30}$H$_{41}$NOW: C, 58.54; H, 6.72; N, 2.27. Found: C, 58.37; H, 6.90; N, 2.39. IR (Nujol): ν_{NO} 1551 cm^{-1}. Low-resolution mass spectrum (probe temperature 120 °C): m/z 615 [P]$^+$. ^{1}H NMR (C$_6$D$_6$): δ 7.49 (d, 4 H, J_{HH} = 7.5 Hz, ortho H), 7.22 (t, 4 H, J_{HH} = 7.5 Hz, meta H), 7.05 (t, 2 H, J_{HH} = 7.5 Hz, para H), 2.95 (d, 2 H, J_{HH} = 11.5 Hz, CH_aH$_x$), 1.72 (s, 6 H, C(CH_3)$_2$), 1.65 (s, 6 H, C(CH_3)$_2$), 1.37 (s, 15 H, C$_5$(CH_3)$_5$), −0.42 (d, 2 H, J_{HH} = 11.5 Hz, CH$_a$$H_x$).

X-ray Crystallographic Analyses of Cp*M(NO)(*o*-tolyl)$_2$ (3) and Cp*W(NO)(*o*-tolyl)$_2$ (6). The X-ray structure determinations of both complexes were performed in a similar manner. A suitable crystal of each compound was obtained by slow cooling of appropriate saturated solutions of each complex, i.e. Et$_2$O for **3** and CH$_2$Cl$_2$/pentane for **6**. Each crystal was mounted in a thin-walled glass capillary under N$_2$ and transferred to a Rigaku AFC6S diffractometer equipped with graphite-monochromated Mo Kα radiation ($\lambda_{K\alpha}$ = 0.710 69 Å). Final unit-cell parameters for each complex were obtained by least-squares analysis of setting angles for 25 reflections, $27.6 \leq 2\theta \leq 35.5°$ for **3** and $22.7 \leq 2\theta \leq 31.9°$ for **6**. The intensities of three standard reflections were measured every 200 reflections during the data collections. The intensities of the standard reflections of **3** and **6** showed linear 25% and 27% decreases with time, respectively, and so the data were scaled for this deterioration in crystal quality. The data were corrected for Lorentz and polarization effects and for absorption using the azimuthal scan method.[20] Pertinent crystallographic and experimental parameters for the two complexes are summarized in Table IV.

Interpretation of the Patterson function yielded the coordinates of the heaviest atoms in each structure, and the full structures of both compounds were then derived by conventional electron density methods and refined by full-matrix least-squares methods on F, minimizing the function $w(|F_o| - |F_c|)^2$, where $w = 4F_o^2/\sigma^2(F_o)^2$. Compounds **3** and **6** are isomorphous and isostructural. Hydrogen atoms were placed in idealized positions on the basis of difference maps, with thermal parameters $B = 1.2B$(bonded atom), and were not refined but were repositioned after each cycle. Final refinements were carried out with non-hydrogen atoms being permitted anisotropic thermal motion. Complex neutral atom scattering factors (for all atoms) and anomalous scattering corrections for the non-hydrogen atoms were taken from ref 21. Final positional and equivalent isotropic parameters for the complexes are given in Table V, and selected bond lengths (Å) and bond angles (deg) are listed in Tables VI and VII. Anisotropic thermal

---

(20) TEXSAN/TEXRAY structure analysis package which includes versions of the following: MITHRIL, integrated direct methods, by C. J. Gilmore; DIRDIF, direct methods for difference structures, by P. T. Beurskens; ORFLS, full-matrix least-squares, and ORFFE, functions and errors, by W. R. Busing, K. O. Martin, and H. A. Levy; ORTEP II, illustrations, by C. K. Johnson.

(21) *International Tables for X-ray Crystallography*; Kynoch Press: Birmingham, England, 1974; Vol. IV, Tables 2.2B and 2.3.1.

Table IV. Crystallographic and Experimental Data[a] for the Complexes Cp*Mo(NO)(*o*-tolyl)$_2$ (3) and Cp*W(NO)(*o*-tolyl)$_2$ (6)

complex	3	6
color	purple	violet
formula	$C_{24}H_{29}NOMo$	$C_{24}H_{29}NOW$
fw	443.44	531.35
cryst syst	monoclinic	monoclinic
space group	$P2_1/a$ (No. 14)	$P21/a$ (No. 14)
a, Å	11.570 (2)	11.612 (3)
b, Å	10.128 (3)	10.168 (5)
c, Å	18.439 (4)	18.250 (3)
α, deg	90	90
β, deg	92.50 (2)	91.87 (2)
γ, deg	90	90
V, Å^3	2158.5 (9)	2154 (1)
Z	4	4
d_{calcd}, Mg/m^{-3}	1.364	1.639
$F(000)$	920	1048
μ(Mo Kα), cm^{-1}	6.04	54.89
T, K	293	293
cryst dimens, mm^3	0.030 × 0.300 × 0.400	0.200 × 0.300 × 0.400
transmissn factors	0.88–1.02	0.80–1.00
scan type	ω–2θ	ω–2θ
scan range, deg	$1.21 + 0.35 \tan \theta$	$1.05 + 0.35 \tan \theta$
scan speed, deg/min	32.0	16.0
2θ limits, deg	$0 \leq 2\theta \leq 60.0$	$0 \leq 2\theta \leq 60.1$
data collected	$+h,+k,\pm l$	$+h,+k,\pm l$
no. of unique rflns	6647	6632
no. of rflns with $I > 3\sigma(I)$	3387	3019
no. of variables	244	245
R_F[b]	0.030	0.037
R_{wF}[c,d]	0.033	0.040
goodness of fit[e]	1.49	1.37
max Δ/σ (final cycle)	0.001	0.05
residual density, e/Å^3	−0.36 to +0.32	−1.18 to +1.05

[a] Rigaku AFCF6 diffractometer, Mo Kα radiation, graphite monochromator. [b] $R_F = \sum||F_o| - |F_c||/\sum|F_o|$. [c] $R_{wF} = [\sum w(|F_o| - |F_c|)^2/\sum F_o^2]^{1/2}$. [d] $w = 4F_o^2/\sigma^2(F_o)^2$. [e] $\text{GOF} = [\sum w(|F_o| - |F_c|)^2/(\text{no. of degrees of freedom})]^{1/2}$.

Table V. Final Positional and Equivalent Isotropic Thermal Parameters (Å^2) for Cp*Mo(NO)(*o*-tolyl)$_2$ (3) and Cp*W(NO)(*o*-tolyl)$_2$ (6)

atom	x	y	z	B_{eq}[a]
		Compound 3		
Mo(1)	0.63205 (2)	0.52448 (2)	0.25028 (1)	3.34 (1)
O(1)	0.8461 (2)	0.3897 (3)	0.2106 (1)	6.8 (1)
N(1)	0.7662 (2)	0.4597 (3)	0.2274 (1)	4.5 (1)
C(1)	0.5583 (3)	0.3222 (3)	0.2806 (2)	4.7 (2)
C(2)	0.4878 (2)	0.4126 (3)	0.3181 (2)	4.2 (1)
C(3)	0.4233 (2)	0.4876 (2)	0.2655 (2)	4.1 (1)
C(4)	0.4525 (3)	0.4428 (3)	0.1959 (2)	4.5 (2)
C(5)	0.5354 (3)	0.3415 (3)	0.2053 (2)	4.7 (2)
C(6)	0.6329 (3)	0.2158 (4)	0.3139 (3)	7.2 (2)
C(7)	0.4716 (3)	0.4181 (4)	0.3987 (2)	6.3 (2)
C(8)	0.3320 (3)	0.5872 (4)	0.2804 (2)	5.9 (2)
C(9)	0.3937 (4)	0.4853 (4)	0.1254 (2)	7.0 (2)
C(10)	0.5818 (4)	0.2563 (4)	0.1460 (3)	7.8 (3)
C(11)	0.6143 (3)	0.6590 (3)	0.1620 (2)	4.0 (1)
C(12)	0.6642 (3)	0.6674 (4)	0.0945 (2)	4.8 (2)
C(13)	0.6483 (3)	0.7828 (5)	0.0526 (2)	6.1 (2)
C(14)	0.5868 (4)	0.8865 (4)	0.0782 (2)	6.7 (2)
C(15)	0.5377 (3)	0.8813 (4)	0.1433 (3)	6.3 (2)
C(16)	0.5492 (3)	0.7685 (3)	0.1837 (2)	5.0 (2)
C(17)	0.6881 (2)	0.6036 (3)	0.3540 (2)	4.0 (1)
C(18)	0.7920 (3)	0.5845 (4)	0.3964 (2)	4.7 (2)
C(19)	0.8187 (3)	0.6712 (4)	0.4533 (2)	5.9 (2)
C(20)	0.7506 (3)	0.7755 (5)	0.4693 (2)	6.6 (2)
C(21)	0.6486 (3)	0.7960 (4)	0.4300 (2)	5.7 (2)
C(22)	0.6175 (3)	0.7082 (4)	0.3744 (2)	4.9 (2)
C(23)	0.7317 (4)	0.5567 (4)	0.0647 (2)	6.9 (2)
C(24)	0.8741 (3)	0.4760 (4)	0.3804 (2)	6.5 (2)
		Compound 6		
W(1)	0.13312 (2)	0.47777 (3)	0.24871 (2)	3.39 (1)
O(1)	0.3464 (5)	0.6152 (6)	0.2059 (4)	6.9 (4)
N(1)	0.2648 (5)	0.5455 (6)	0.2241 (4)	4.5 (3)
C(1)	−0.0735 (6)	0.5132 (7)	0.2648 (5)	4.3 (4)
C(2)	−0.0112 (6)	0.5899 (8)	0.3178 (5)	4.3 (4)
C(3)	0.0563 (6)	0.6798 (7)	0.2778 (5)	4.7 (4)
C(4)	0.0352 (7)	0.6587 (8)	0.2027 (5)	4.8 (4)
C(5)	−0.0464 (6)	0.5573 (8)	0.1937 (5)	4.5 (4)
C(6)	−0.1660 (7)	0.411 (1)	0.2804 (6)	6.1 (5)
C(7)	−0.0249 (9)	0.585 (1)	0.3988 (5)	6.7 (6)
C(8)	0.1323 (9)	0.788 (1)	0.3100 (7)	7.9 (7)
C(9)	0.080 (1)	0.741 (1)	0.1408 (7)	7.9 (7)
C(10)	−0.104 (1)	0.510 (1)	0.1246 (6)	7.2 (6)
C(11)	0.1879 (6)	0.3979 (8)	0.3530 (4)	4.2 (4)
C(12)	0.2915 (6)	0.416 (1)	0.3943 (5)	4.7 (4)
C(13)	0.3185 (7)	0.331 (1)	0.4522 (5)	6.1 (5)
C(14)	0.2491 (8)	0.228 (1)	0.4709 (5)	6.6 (6)
C(15)	0.1476 (8)	0.208 (1)	0.4319 (5)	5.9 (5)
C(16)	0.1176 (6)	0.294 (1)	0.3759 (5)	4.8 (4)
C(17)	0.3743 (8)	0.524 (1)	0.3774 (6)	6.5 (5)
C(18)	0.1157 (7)	0.3368 (8)	0.1633 (4)	4.1 (4)
C(19)	0.1660 (7)	0.3258 (8)	0.0941 (5)	4.7 (4)
C(20)	0.1501 (9)	0.213 (1)	0.0520 (5)	6.2 (5)
C(21)	0.0855 (9)	0.110 (1)	0.0771 (6)	6.7 (6)
C(22)	0.0373 (8)	0.115 (1)	0.1448 (6)	6.3 (6)
C(23)	0.0493 (7)	0.2278 (9)	0.1851 (6)	5.3 (5)
C(24)	0.2366 (8)	0.434 (1)	0.0634 (5)	6.6 (5)

[a] $B_{eq} = {}^8/_3\pi^2\sum\sum U_{ij}a_i^*a_j^*(a_i \cdot a_j)$.

parameters, hydrogen parameters, and full listings of molecular dimensions for 3 and 6 are provided as supplementary material. Views of the solid-state molecular structures of complexes 3 and 6 are displayed in Figure 1.

Electrochemical Measurements. The detailed methodology employed for cyclic voltammetry (CV) studies in these laboratories has been outlined elsewhere.[22,23] The potentials were supplied by a BAS CV27 voltammograph, and the resulting cyclic voltammograms were recorded on a Hewlett-Packard Model 7090A measurement plotting system in the buffered recording mode. All measurements were made at room temperature.

The potentials, $E^{\circ\prime}$, are defined as the average of the cathodic and anodic peak potentials, $(E_{p,c} + E_{p,a})/2$, and are reported versus the aqueous saturated calomel electrode (SCE). Solutions were prepared at 0.1 M in the $[n\text{-Bu}_4\text{N}]\text{PF}_6$ support electrolyte and ~6×10^{-4} M in the organometallic complex to be studied. During the course of an electrochemical experiment the solutions were maintained under an atmosphere of N_2. The three-electrode cell consisted of a Pt-bead working electrode (~1 mm diameter), a Pt-wire auxiliary electrode, and a SCE in a separate holder connected to the cell compartment via a Luggin probe separated by a frit. Compensation for *iR* drop in potential measurements was not employed during this study. Ferrocene (Fc) was used as an internal reference in these studies, with the redox couple, Fc/Fc$^+$, occurring at $E^{\circ\prime} = 0.54$ V versus SCE in THF over the range of scan rates (v) used (0.10–0.80 V s^{-1}). The anodic and cathodic peak separation (ΔE) for this couple increases with increasing scan rate (80–240 mV between 0.10 and 0.80 V s^{-1}), but since the Fc/Fc$^+$ couple is known to be highly reversible, other redox couples exhibiting peak separations similar to that of the internal standard were also considered to be electrochemically reversible. The ratio of cathodic peak current to anodic peak current, $i_{p,c}/i_{p,a}$, for the oxidation of Fc was unity over all scan rates used, as expected for a chemically reversible process. The linearity of a plot of $i_{p,a}$ vs $v^{1/2}$ was checked for all reduction processes to establish the presence of diffusion control.

Results and Discussion

Synthetic Methodology. We have previously established that the dichloro complexes Cp'M(NO)Cl$_2$ (M = Mo, W) are superior to their iodo analogues as synthetic pre-

---

(22) Herring, F. G.; Legzdins, P.; Richter-Addo, G. B. *Organometallics* **1989**, *8*, 1485.

(23) Legzdins, P.; Wassink, B. *Organometallics* **1984**, *3*, 1811.

Table VI. Selected Bond Lengths (Å) with Esd's in Parentheses for Cp*Mo(NO)(*o*-tolyl)$_2$ (3) and Cp*W(NO)(*o*-tolyl)$_2$ (6)

3		6	
Mo(1)-N(1)	1.754 (2)	W(1)-N(1)	1.749 (6)
Mo(1)-C(1)	2.298 (3)	W(1)-C(1)	2.453 (7)
Mo(1)-C(2)	2.412 (3)	W(1)-C(2)	2.415 (7)
Mo(1)-C(3)	2.472 (3)	W(1)-C(3)	2.308 (7)
Mo(1)-C(4)	2.413 (3)	W(1)-C(4)	2.307 (7)
Mo(1)-C(5)	2.300 (3)	W(1)-C(5)	2.423 (7)
Mo(1)-C(11)	2.125 (3)	W(1)-C(11)	2.146 (8)
Mo(1)-C(17)	2.148 (3)	W(1)-C(18)	2.122 (8)
Mo(1)-Cp[a]	1.754 (2)	W(1)-Cp[a]	2.056 (3)
O(1)-N(1)	1.216 (3)	O(1)-N(1)	1.238 (8)

[a] Cp refers to the centroid of the pentamethylcyclopentadienyl ligand.

Table VII. Selected Bond Angles (deg) with Esd's in Parentheses for Cp*Mo(NO)(*o*-tolyl)$_2$ (3) and Cp*W(NO)(*o*-tolyl)$_2$ (6)

3		6	
N(1)-Mo(1)-C(11)	96.5 (1)	N(1)-W(1)-C(11)	98.0 (3)
N(1)-Mo(1)-C(17)	96.8 (1)	N(1)-W(1)-C(18)	98.1 (3)
N(1)-Mo(1)-Cp[a]	119.3 (1)	N(1)-W(1)-Cp[a]	118.2 (2)
C(11)-Mo(1)-C(17)	117.3 (1)	C(11)-W(1)-C(18)	114.4 (3)
C(11)-Mo(1)-Cp[a]	111.0 (1)	C(11)-W(1)-Cp[a]	114.9 (2)
C(17)-Mo(1)-Cp[a]	114.40 (9)	C(18)-W(1)-Cp[a]	111.6 (2)
Mo(1)-N(1)-O(1)	166.0 (2)	W(1)-N(1)-O(1)	168.0 (6)
Mo(1)-C(11)-C(12)	133.7 (2)	W(1)-C(11)-C(12)	130.4 (6)
Mo(1)-C(11)-C(16)	108.8 (2)	W(1)-C(11)-C(16)	112.9 (6)
Mo(1)-C(17)-C(18)	131.0 (2)	W(1)-C(18)-C(19)	132.6 (6)
Mo(1)-C(17)-C(22)	111.3 (2)	W(1)-C(18)-C(23)	111.3 (6)

[a] Cp refers to the centroid of the pentamethylcyclopentadienyl ligand.

cursors for the preparation of Cp'M(NO)(alkyl)$_2$ complexes.[3,22,24-26] Consequently, the Cp'M(NO)Cl$_2$ complexes are now used exclusively as starting materials in our work.

Previous electrochemical investigations showed that the metathesis reactions forming dialkyl nitrosyl complexes probably proceed through radical anion intermediates of the type [Cp'M(NO)Cl$_2$]$^{\bullet-}$ (M = Mo, W).[22] Therefore, it was our view that the methodology employed for the preparation of the Cp'M(NO)(aryl)$_2$ complexes should be designed to maximize the stability of these radical anion intermediates. This requirement implies the use of the above-mentioned dichloro nitrosyl starting materials,[22] highly solvating solvents to stabilize the putative ionic intermediates, and low temperatures to avoid possible decomposition pathways of the newly formed organometallics. Gratifyingly, application of these ideas does indeed lead to the successful synthesis of new Cp*M(NO)(aryl)$_2$ complexes. This synthetic route, summarized in eq 5, outlines the choices of reagent, solvent, and temperature that are now routinely used to prepare these highly reactive molecules in our laboratories. The particular advantage of reaction 5 is that dioxane ligates MgCl$_2$ more efficiently than does the oxygen atom of the nitrosyl ligand in Cp*M(NO)(aryl)$_2$, thereby removing the need for water to liberate the diaryls from isonitrosyl adducts of the type [Cp*M(NO)(aryl)$_2$]$_2$·MgCl$_2$ (cf. eq 2).[27] Also, MgCl$_2$·(dioxane) is very insoluble in even moderately polar solvents, thus allowing uncontaminated Cp*M(NO)(aryl)$_2$ complexes to be extracted from the final reaction mixtures.

$$\mathrm{Cp^*M(NO)(Cl)_2} + \mathrm{(aryl)_2Mg\cdot(dioxane)} \xrightarrow{\text{THF, argon, }-50\text{ to }0\ ^\circ\text{C}} \mathrm{Cp^*M(NO)(aryl)_2} + \mathrm{MgCl_2\cdot(dioxane)} \quad (5)$$

The Cp*M(NO)(aryl)$_2$ product complexes are obtainable from reactions 5 as analytically pure, crystalline solids in 32–81% yield. They are thermally stable as solids when analytically pure. Overall, diaryl complexes are markedly less stable than their dialkyl analogues, since they are prone to decompose autocatalytically in the presence of trace amounts of impurities even at low temperatures. The diaryl complexes are soluble in most common organic solvents, but to a noticeably lesser extent than their dialkyl analogues. For instance, Cp*W(NO)(*p*-tolyl)$_2$ is the only diaryl complex that is soluble in hexanes. In general, the *p*-tolyl derivatives are more soluble than the *o*-tolyl derivatives, which in turn are more soluble than the phenyl complexes. Both in solution and in the solid state, the Cp*M(NO)(aryl)$_2$ complexes decompose rapidly when exposed to the atmosphere. The numbering scheme, color, yield, and elemental analysis data for complexes 1–6 are collected in Table I, while their mass spectral, infrared, and ^{1}H NMR data are compiled in Tables II and III.

Spectroscopic Characterization. The spectroscopic properties of the six diaryl complexes are consistent with their possessing monomeric, three-legged piano-stool molecular structures having a 16-valence-electron configuration at the metal center. Thus, just as observed previously for related dialkyl complexes, the ^{1}H NMR spectra of these diaryl complexes (Table III) are not unusual and are fully consistent with their formulations.

The ν_{NO} bands in the IR spectra of the molybdenum diaryl complexes are, on average, some 20 cm^{-1} higher in energy than those of their tungsten congeners. These ν_{NO} bands are also some 30–50 cm^{-1} lower in energy than those exhibited by the corresponding dichloro complexes, a manifestation of the better electron donation from an aryl ligand than from an electronegative chloro ligand. However, when the IR spectra of the diaryl complexes are compared to those of the dialkyl complexes, it is obvious that aryl ligands are considerably less electron-donating than alkyl ligands. Both the solution and solid-state IR spectra of the dialkyl derivatives display ν_{NO} values which are 10–30 cm^{-1} lower in energy than those of similar diaryl complexes. In other words, their IR spectroscopic properties imply that in the Cp*M(NO)(aryl)$_2$ complexes the metal centers are more electron-deficient than in their alkyl analogues, and this in turn is manifested by the molybdenum and tungsten centers in the aryl species being more Lewis acidic than in related Cp*M(NO)(alkyl)$_2$ complexes.

Attempts to prepare the Cp-containing members of this class of complexes by reaction 5 indicate that the desired diaryl products are indeed formed in solution. This conclusion is supported by the observation of a single ν_{NO} band in the IR spectra of the final reaction mixtures at values consistent with those expected for diaryl complexes. Furthermore, the reaction solutions are a very distinctive blue to purple color which is characteristic of isolable diaryl nitrosyl complexes. However, all attempts to isolate the Cp–containing products from these solutions have been unsuccessful so far, the decomposition of the desired products being indicated by the loss of the characteristic

---

(24) Dryden, N. H. Ph.D. Dissertation, The University of British Columbia, 1990.

(25) Veltheer, J. E.; Legzdins, P. In *Handbuch der Präparativen Anorganischen Chemie*, 4th ed.; Herrmann, W. A., Ed.; Thieme-Verlag: Stuttgart, Germany, in press.

(26) (a) Dryden, N. H.; Legzdins, P.; Phillips, E. C.; Trotter, J.; Yee, V. C. *Organometallics* **1990**, *9*, 882. (b) Legzdins, P.; Jones, R. H.; Phillips, E. C.; Yee, V. C.; Trotter, J.; Einstein, F. W. B. *Organometallics* **1991**, *10*, 986. (c) Dryden, N. H.; Legzdins, P.; Trotter, J.; Yee, V. C. *Organometallics* **1991**, *10*, 2857.

(27) The reactions of typical Cp*M(NO)(aryl)$_2$ complexes with water have been addressed elsewhere.[9,10]

colors of the reaction mixtures upon attempted workup. Additionally, in situ generated CpMo(NO)(aryl)$_2$ when reacted with PMe$_3$ does not yield the 18-electron adduct CpMo(NO)(aryl)$_2$(PMe$_3$).

Our inability to isolate CpW(NO)(aryl)$_2$ complexes other than CpW(NO)(*o*-tolyl)$_2$[10] was unexpected, since numerous CpW(NO)(alkyl)$_2$ complexes have been isolated in our laboratories. Since the Cp*-containing analogues are accessible, however, it may be that a planar aromatic ligand in conjunction with the less sterically demanding Cp group does not shield the unsaturated metal center as well as do bulky alkyl and Cp* ligands. Our recent discovery of the thermal instability of CpMo(NO)(CH$_2$CMe$_3$)$_2$[28] indicates to us that CpMo(NO)(aryl)$_2$ species could also be quite thermally sensitive, particularly if a low-activation-energy pathway for their decomposition exists. Evidently, the additional steric shielding and greater electron-donating ability of the Cp* ligand versus the Cp ligand provide the additional factors necessary to render the Cp*M(NO)(aryl)$_2$ product complexes stable enough to be isolated. This general stabilizing ability of the Cp* group has also been documented for other systems.[29]

X-ray Crystallographic Analyses of Complexes 3 and 6. The solid-state molecular structures of both Cp*M(NO)(*o*-tolyl)$_2$ complexes have been established, and their monomeric natures have been confirmed. The intramolecular geometrical parameters of both molecules are presented in Tables VI and VII, and they resemble those found in CpW(NO)(CH$_2$SiMe$_3$)$_2$.[5] The chemically most interesting feature of both diaryl structures is the apparent size of the open coordination site at their metal centers. Thus, while in CpW(NO)(CH$_2$SiMe$_3$)$_2$ the C$_{\text{alkyl}}$–W–C$_{\text{alkyl}}$ bond angle is 109.6 (4)°, the C$_{\text{aryl}}$–M–C$_{\text{aryl}}$ bond angles in the Cp*M(NO)(*o*-tolyl)$_2$ complexes are 117.3 (1)° (M = Mo) and 114.4 (3)° (M = W). Furthermore, it is also evident from the structures of **3** and **6** that the σ-bonded aryl groups are considerably less sterically demanding than are similarly attached bulky alkyl groups. Thus, the nonbonded separation between the methylene carbons of CpW(NO)(CH$_2$SiMe$_3$)$_2$ of 3.44 Å is somewhat smaller than the ipso carbon separation of 3.65 Å (for **3**) and 3.59 Å (for **6**). In other words, the metal centers in **3** and **6** are relatively more electron-deficient (shown by their IR properties) and more accessible to attacking nucleophiles (established by their structures) than those in their dialkyl analogues. This feature is also manifested by the characteristic properties of these complexes which are considered in the next section.

Reactivity Patterns of the Diaryl Complexes. In all cases investigated to date, the diaryl complexes react with substrates orders or magnitude faster than analogous dialkyl complexes under similar conditions, e.g. eqs 6 and 7. The transformation shown in eq 6 involves CO insertion

$$\text{Cp*W(NO)}(p\text{-tolyl})_2 + \text{CO (1 atm, 25 °C)} \rightarrow \text{Cp*W(NO)(C\{O\}-}p\text{-tolyl)}(p\text{-tolyl}) \quad (6)$$

$$\text{CpW(NO)}(p\text{-tolyl})_2 + \text{S}_8 \text{ (25 °C)} \rightarrow \text{CpW(NO)(S-}p\text{-tolyl)}_2 \quad (7)$$

to form an acyl complex. It is very facile, being complete in a matter of seconds under ambient conditions.[30] In comparison, Cp*W(NO)(CH$_2$CMe$_2$Ph)$_2$ reacts with CO to form the analogous monoacyl complex only after 6 h under the same reaction conditions.[30] In a similar manner, in situ generated CpW(NO)(*p*-tolyl)$_2$ reacts instantaneously with elemental sulfur in nonpolar solvents at 25 °C to provide CpW(NO)(S-*p*-tolyl)$_2$.[31] In contrast, CpW(NO)(CH$_2$SiMe$_3$)$_2$ reacts with sulfur in toluene (50 °C) over a period of 1 day in a sequential manner to form first CpW(NO)(SCH$_2$SiMe$_3$)(CH$_2$SiMe$_3$), then CpW(NO)(η^2-S$_2$CH$_2$SiMe$_3$)(CH$_2$SiMe$_3$), and finally CpW(NO)(SCH$_2$SiMe$_3$)$_2$.[5,32]

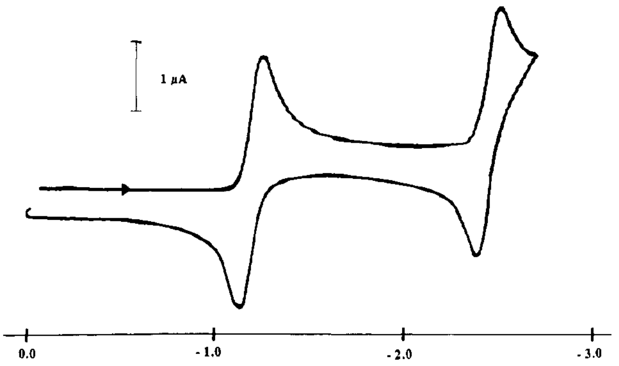

Figure 2. Ambient-temperature cyclic voltammogram of complex **5** (5×10^{-4} M) in THF containing 0.10 M [*n*-Bu$_4$N]PF$_6$ measured at a platinum-bead electrode with a scan rate of 400 mV s^{-1}.

The diaryl complexes are also more potent Lewis acids than are the analogous dialkyl species. Thus, previous work has demonstrated that CpW(NO)(CH$_2$SiMe$_3$)$_2$ and PMe$_3$ establish an equilibrium in toluene at room temperature,[5] i.e.

$$\text{CpW(NO)(CH}_2\text{SiMe}_3)_2 + \text{PMe}_3 \rightleftarrows \text{CpW(NO)(CH}_2\text{SiMe}_3)_2(\text{PMe}_3) \quad (8)$$

Hence, the monophosphine adduct CpW(NO)(CH$_2$SiMe$_3$)$_2$(PMe$_3$) can only be isolated in the presence of an excess of PMe$_3$, and it loses PMe$_3$ slowly when exposed to vacuum. In contrast, the analogous equilibrium between PMe$_3$ and Cp*W(NO)(*p*-tolyl)$_2$ lies completely to the right as portrayed in eq 9. Prolonged exposure or isolated complex **7** to high vacuum (10^{-6} Torr) for days at room temperature does not regenerate complex **5**.

$$\underset{\mathbf{5}}{\text{Cp*W(NO)}(p\text{-tolyl})_2} + \text{PMe}_3 \rightarrow \underset{\mathbf{7}}{\text{Cp*W(NO)}(p\text{-tolyl})_2(\text{PMe}_3)} \quad (9)$$

Electrochemical Properties of Complex 5. Knowledge of the redox properties of the diaryl complexes is of fundamental importance to understanding their reactivity behavior. Hence, Cp*W(NO)(*p*-tolyl)$_2$ (**5**) has been investigated by cyclic voltammetry as a representative member of the diaryl class of compounds. The cyclic voltammogram of **5** in THF (Figure 2) exhibits reduction features consistent with the occurrence of two reversible, one-electron reductions (eq 10) at $E^{\circ\prime}$ values of −1.21 and −2.46 V. The cyclic voltammogram of **5** is devoid of any oxidation features out to the solvent limit of about 0.8 V.

$$\text{Cp*W(NO)}(p\text{-tolyl})_2 \underset{-e^-}{\overset{+e^-}{\rightleftarrows}} [\text{Cp*W(NO)}(p\text{-tolyl})_2]^{\bullet -} \underset{-e^-}{\overset{+e^-}{\rightleftarrows}} [\text{Cp*W(NO)}(p\text{-tolyl})_2]^{2-} \quad (10)$$

---

[28] Legzdins, P.; Rettig, S. J.; Veltheer, J. E. *J. Am. Chem. Soc.*, submitted for publication.

[29] Gambarotta, S.; Floriani, C.; Chiesi-Villa, A.; Guastini, C. *Inorg. Chem.* **1984**, *23*, 1739 and references cited therein.

[30] Complete details of the reactions of various Cp′M(NO)R$_2$ complexes (Cp′ = Cp, Cp*; M = Mo, W; R = alkyl, aryl, benzyl) with CO (low and high pressures) are discussed in a forthcoming paper: Batchelor, R. J.; Dryden, N. H.; Einstein, F. W. B.; Legzdins, P.; Lundmark, P. J. Manuscript in preparation.

[31] Legzdins, P.; Ross, K. J. Unpublished observations.

[32] Evans, S. V.; Legzdins, P.; Rettig, S. J.; Sánchez, L.; Trotter, J. *Organometallics* **1987**, *6*, 7.

Table VIII. Electrochemical Data for the First Reductions of $Cp^*W(NO)(p\text{-tolyl})_2$ and $Cp^*W(NO)(CH_2CMe_2Ph)_2$[a]

scan rate (v), V s^{-1}	$E^{\circ\prime}_1$,[b] V	ΔE[c]	$i_{p,a}/i_{p,c}$[d]
	$Cp^*W(NO)(p\text{-tolyl})_2$		
0.80	−1.21	0.13 (0.14)	1.0
0.40	−1.21	0.10 (0.10)	1.0
0.20	−1.21	0.08 (0.10)	1.0
0.10	−1.21	0.07 (0.08)	1.0
	$Cp^*W(NO)(CH_2CMe_2Ph)_2$		
0.80	−1.62	0.25 (0.24)	1.0
0.40	−1.62	0.19 (0.19)	1.0
0.20	−1.62	0.16 (0.16)	1.0
0.10	−1.62	0.13 (0.13)	1.0

[a] In THF containing 0.10 M $[n\text{-Bu}_4N]PF_6$, at a Pt-bead working electrode. Potentials are measured vs SCE. [b] Defined as the average of the cathodic and anodic peak potentials (±0.02 V). [c] Defined as the separation of the cathodic and anodic peak potentials. Values of ΔE given in brackets are for the Cp_2Fe/Cp_2Fe^+ couple under the same conditions. [d] Ratio of anodic peak current to cathodic peak current.

The linearity of plots of $i_{p,a}$ vs $v^{1/2}$ for these reduction waves show that the reductions are diffusion-controlled. Comparisons of the ΔE values for these reductions with the internal Fc/Fc^+ reference indicate that the first reductions are electrochemically reversible. The $i_{p,a}/i_{p,c}$ value for the first reduction is unity over the range of scan speeds used, thereby establishing its chemical reversibility.

Electrochemical data for the first reversible reductions of $Cp^*W(NO)(p\text{-tolyl})_2$ and $Cp^*W(NO)(CH_2CMe_2Ph)_2$ are tabulated for comparison in Table VIII. Interestingly, $Cp^*W(NO)(p\text{-tolyl})_2$ is easier to reduce by 410 mV than is $Cp^*W(NO)(CH_2CMe_2Ph)_2$, which exhibits a reversible first reduction in THF at −1.62 V. This result is consistent with the diaryl complex containing a more electron-deficient metal center than does the related $Cp^*W(NO)(\text{alkyl})_2$ species. Hence, the aryl ligands of $Cp^*W(NO)(\text{aryl})_2$ evidently reduce the electron density at the metal center, allowing such complexes to accept electrons more easily than analogous $Cp^*W(NO)(\text{alkyl})_2$ complexes.

If the LUMO of $Cp^*W(NO)(p\text{-tolyl})_2$ is indeed a metal-centered orbital, as it is on the model complex $CpW(NO)Me_2$ (vide supra), the diaryl complex should exhibit a second reversible reduction at a potential more negative than −1.21 V. Such a chemically and electrochemically reversible reduction does indeed occur at −2.46 V. From Figure 2 and the data presented in Table IX, it is apparent that an accurate determination of $i_{p,a}/i_{p,c}$ for this feature is not possible, but the reduction wave *is* electrochemically reversible and in all likelihood is chemically reversible as well. Some of the $[Cp^*W(NO)(p\text{-tolyl})_2]^{2-}$ formed in the second reduction may react with $Cp^*W(NO)(p\text{-tolyl})_2$ to give two molecules of $[Cp^*W(NO)(p\text{-tolyl})_2]^{\bullet-}$ before reoxidizing to $[Cp^*W(NO)(p\text{-tolyl})_2]^{\bullet-}$ electrochemically. The second reduction of $Cp^*W(NO)(CH_2CMe_2Ph)_2$ in THF apparently occurs beyond the solvent limit of ∼−2.7 V, thereby precluding a comparison of this feature with that exhibited by the $Cp^*W(NO)(p\text{-tolyl})_2$ complex.

Table IX. Electrochemical Data for the Second Reduction of $Cp^*W(NO)(p\text{-tolyl})_2$[a]

scan rate (v), V s^{-1}	$E^{\circ\prime}_2$,[b] V	ΔE[c]	$i_{p,a}/i_{p,c}$[d]
0.80	−2.46	0.12 (0.14)	0.8[e]
0.40	−2.46	0.10 (0.10)	0.8[e]
0.20	−2.46	0.07 (0.10)	0.8[e]
0.10	−2.46	0.06 (0.08)	0.8[e]

[a] In THF containing 0.10 M $[n\text{-Bu}_4N]PF_6$, at a Pt-bead working electrode. Potentials are measured vs SCE. [b] Defined as the average of the cathodic and anodic peak potentials (±0.02 V). [c] Defined as the separation of the cathodic and anodic peak potentials. Values of ΔE given in brackets are for the Cp_2Fe/Cp_2Fe^+ couple under the same conditions. [d] Ratio of anodic peak current to cathodic peak current. [e] Accurate determination of this ratio was not possible since the reduction wave occurred very close to the solvent limit of the THF/TBAH electrolyte system.

Epilogue

In addition to developing a reliable synthetic route to various $Cp^*M(NO)(\text{aryl})_2$ complexes from their $Cp^*M(NO)Cl_2$ precursors, this work has established some fundamental facts about the diaryl species vis-à-vis their better known alkyl analogues. Specifically, the thermal stability of $Cp'M(NO)R_2$ complexes appears to be Cp* > Cp, alkyl > aryl, and W > Mo. Hence, $CpMo(NO)(\text{aryl})_2$ complexes have yet to be isolated. Furthermore, the investigations presented in this paper have established that the diaryl complexes are more reactive than their dialkyl counterparts, principally because their metal centers are more electron-deficient and sterically more accessible to incoming nucleophilic reactants. Finally, electrochemical investigations of $Cp^*W(NO)(p\text{-tolyl})_2$ have established that its reduction behavior is consistent with the view that the Fenske–Hall MO description of the bonding in $CpMo(NO)Me_2$ may also be extended to encompass $Cp^*M(NO)(\text{aryl})_2$ complexes. The electrochemical existence of $[Cp^*W(NO)(p\text{-tolyl})_2]^{\bullet-}$ and $[Cp^*W(NO)(p\text{-tolyl})_2]^{2-}$ implies that it might be possible to prepare and structurally characterize these latter species. The molecular structures of the mono- and dianions would also be of interest, since the neutral diaryl compounds and their reduced forms should be essentially isostructural if the additional electrons are being accommodated in a metal-centered, nonbonding orbital. Suffice it to say that these and other reactivity studies with the diaryl species prepared in this work are continuing.

Acknowledgment. We are grateful to the Natural Sciences and Engineering Research Council of Canada for support of this work in the form of grants to P.L. and a postgraduate scholarship to N.H.D.

Supplementary Material Available: Tables of hydrogen atom coordinates, anisotropic thermal parameters, all bond lengths and bond angles, torsion angles, intermolecular distances, and least-squares planes for complexes 3 and 6 (29 pages). Ordering information is given on any current masthead page.

OM920054K